

Chapter 7

Prediction of functional recovery after revascularization in patients with chronic ischemic myocardial dysfunction: perfusable tissue index by positron emission tomography and contrast-enhanced MRI comparison study

Olga Bondarenko

Paul Knaapen

Aernout M. Beek

Ronald Boellaard

Adriaan A. Lammertsma

Albert C. van Rossum

ABSTRACT

Objectives

In patients with chronic ischemic myocardial dysfunction perfusable tissue index (PTI), obtained with positron emission tomography, using oxygen-15-labeled water and carbon monoxide as tracers, is inversely related to the extent of myocardial scar (non-perfusable tissue). Delayed contrast-enhanced (DCE) MRI accurately depicts the regional extent of myocardial fibrosis and predicts functional recovery after revascularization in patients with ischemic cardiomyopathy. Our aim was to compare PTI as a viability marker with DCE MRI.

Methods

Fourteen patients with ischemic LV dysfunction were studied with positron emission tomography, using oxygen-15-labeled water and carbon monoxide as tracers, and with contrast-enhanced MRI.

Results

Functional improvement occurred in 38 of initially dysfunctional, revascularized segments (56%). Mean PTI was 1.04 ± 0.20 in the improved segments vs. 0.85 ± 0.21 in the group without functional improvement ($p < 0.001$). The areas under the ROC curves (AUC's) of PTI and DCE MRI were 0.7 and 0.74, respectively ($p = \text{NS}$). Cut-off value of 25% DCE allowed correct identification of 82% segments with and 64% segments without reversible dysfunction. A threshold of 0.89 for PTI yielded the best diagnostic accuracy with sensitivity and specificity values of 76% and 54%, respectively.

Conclusion

PTI can identify viable myocardium and predict improvement in regional function after revascularization in patients with chronic ischemic LV dysfunction. Its diagnostic accuracy is comparable with DCE MRI.

INTRODUCTION

Identification of viable myocardium in patients with ischemic cardiomyopathy is of great clinical importance, as patients with evidence of myocardial viability will benefit from revascularization¹.

Delayed contrast-enhanced magnetic resonance imaging (DCE MRI) is a well-established tool for myocardial viability testing. It visualizes injured myocardium with high spatial resolution². Several studies have demonstrated effectiveness of this technique in predicting functional recovery after revascularization in patients with chronic ischemic left ventricular (LV) dysfunction³⁻⁶.

The perfusable tissue index (PTI) is an alternative method for detection of myocardial viability⁷⁻¹¹. PTI reflects the fraction of the myocardium that is able to exchange water rapidly, i.e. perfusable by water. PTI is a positron emission tomography (PET) derived index, in which the water perfusable tissue fraction (PTF) is related to the anatomic tissue fraction (ATF). Assuming the non-perfused fraction to be scar tissue, the reduction of PTI is a measure of the extent of damaged myocardium. Dysfunctional myocardium with normal or near normal PTI is expected to be viable because the amount of scar tissue is limited. In contrast, dysfunctional myocardium with a significant reduced PTI is less likely to be viable because more scar tissue is present.

In a previously published report¹² we demonstrated that PTI is inversely related to the extent of scar tissue, estimated by DCE-MRI, in patients with chronic ischemic LV dysfunction. A PTI cutoff value of 0.89 yielded the best diagnostic accuracy for detection of myocardial viability, when taking DCE-MRI as a reference. However, recovery of myocardial function after revascularization was not assessed. This cutoff value of 0.89 is distinctly higher than the optimal threshold of 0.70 observed in prior studies^{7;8;10}.

Therefore, our aim was to compare PTI as a viability marker with DCE-MRI in patients with chronic ischemic cardiomyopathy, using functional recovery after revascularization (measured by MRI) as a reference to establish the diagnostic accuracy of PTI as a viability marker and determine the optimal cutoff value.

METHODS

Patient population

Fourteen patients with chronic ischemic LV dysfunction, who were scheduled to undergo surgical or percutaneous revascularization, were included. They underwent PET and baseline MRI one month before and follow-up MRI six months after revascularization. Exclusion criteria were any absolute or relative contraindication to PET or MRI (e.g. pacemaker, claustrophobia, atrial fibrillation). Baseline characteristics of the patient population are given in Table 1. The protocol was approved by the Medical Ethics Committee of the VU University Medical Center, and all patients gave written informed consent.

Percutaneous coronary intervention (PCI) was performed in half of the patients. Complete revascularisation was defined as revascularisation of all major epicardial vessels or first generation side branches with >50% diameter stenosis. For patients in whom revascularisation was incomplete, only segments in revascularized coronary artery territories were considered. All patients were in stable clinical condition at the time of the imaging and there was no clinical evidence of ischemic events in the period between the different examinations and revascularization.

Table 1. Baseline patient characteristics.

Males/females (n)	11 / 3
Age (yrs)	62 ± 13
Coronary angiography (n)	
Single-vessel disease	3
Two-vessel disease	3
Three-vessel disease	8
History of myocardial infarction (n)	9
Previous revascularization (n)	
CABG	0
PCI	2
LVEF (%)	34 ± 12
LVEDVI (mL/m ²)	129 ± 40
LVESVI (mL/m ²)	88 ± 42

CABG = Coronary Artery Bypass Grafting. PCI = Percutaneous Coronary Intervention. LVEF = Left Ventricular Ejection Fraction. LVEDVI = Left Ventricular End-Diastolic Volume Indexed (to body surface area). LVESVI = Left Ventricular End-Systolic Volume Indexed.

Imaging protocols

Positron Emission Tomography. All scans were performed in 2D mode, using an ECAT EXACT HR+ (Siemens/CTI, Knoxville, Tenn., USA). The scanning protocol was identical to that described previously¹³. Briefly, after a transmission scan, 1100 MBq of H₂¹⁵O was injected intravenously as a bolus injection. A dynamic scan was acquired for duration of 10 minutes. During a two minute period subjects inhaled at least 2000 MBq of C¹⁵O and a single frame was acquired for duration of 6 minutes, starting one minute after the end of inhalation to allow for equilibration in the blood pool. During the C¹⁵O scan three venous blood samples were drawn from the intravenous line and counted in a sodium iodide well-counter cross calibrated against the scanner.

Magnetic Resonance Imaging. Magnetic resonance imaging was performed on a 1.5 Tesla scanner (Sonata, Siemens, Erlangen, Germany), using a four-element phased-array body radiofrequency receiver coil. All images were acquired with electrocardiogram gating and during repeated breath-holds of 10 to 15 seconds, depending on heart rate. After localizing scouts, cine images were acquired using a segmented steady-state-free precession sequence in three long axis views (two-, three, and four-chamber view) and in multiple short-axis views with a slice distance of 10 mm, covering the whole LV from base to apex. Scan parameters were: temporal resolution 34 ms, TR 3.0 ms. TE 1.5 ms, typical voxel size 1.4 X 1.8 X 5 mm³. Contrast-enhanced images were acquired 15 to 20 minutes after intravenous administration of 0.2 mmol/kg gadolinium-DTPA in the same view used as cine CMR, using a two-dimensional segmented inversion-recovery prepared gradient-echo sequence (TE 4.4 ms, TR 9.8 ms, inversion time 250 to 300 ms, typical voxel size 1.3 X 1.6 X 5 mm³).

Data analysis

Positron Emission Tomography. Anatomical tissue fraction images were generated according to the procedure described by Iida et al¹⁴. Transaxial ATF images of the left ventricle were reoriented according to the anatomic axis of the heart and slices were displayed as short-axis slices. The same reslicing parameters were applied to the dynamic H₂¹⁵O images. ROIs were defined manually at the basal and midventricular level of the left ventricle as previously described. Corresponding ROIs from a variable number of slices were grouped in each patient to generate twelve volumes of interest (6 basal and 6

midventricular). The inferior volumes of interest were excluded from analysis because of anticipated perfusable tissue fraction spillover effects from the liver¹³.

Additional ROIs were defined in the left atrium and right ventricular chamber. This set of ROIs was projected on the dynamic H₂¹⁵O images in order to generate image derived input functions. Using the standard single tissue compartment model together with these input functions, myocardial blood flow in perfusable tissue (MBF_p) (mL • min⁻¹ • mL⁻¹) and PTF (mL • mL⁻¹) were determined for all myocardial tissue time activity curves. Corrections were made for spillover from both the left and right ventricle using the method described by Hermansen et al¹⁵. PTI was obtained by dividing PTF by ATF.

Magnetic Resonance Imaging. The same regions on the short axis slices were defined as described above. Each myocardial segment was evaluated for the presence of hyperenhancement, defined as an area of signal enhancement > 5 SD of the signal of non-enhanced myocardium¹⁶. The total myocardial area and contrast-enhanced area per sector were traced manually. The extent of contrast enhancement was expressed as a percentage of the total myocardial area studied. Additionally, segmental end-diastolic wall thickness (EDWT) and wall thickening were determined by manual tracing of endocardial and epicardial borders in end-diastolic and end-systolic images, excluding trabeculations and papillary muscles.

Assessment of regional and global function. Segmental wall thickness was measured at end-systole and end-diastole by the modified centerline method¹⁷ after manual tracing of endocardial and epicardial borders in stop-frame images, excluding trabeculae and papillary muscles. Segmental wall thickening (SWT) in millimeters was calculated as: end systolic wall thickness minus end diastolic wall thickness. Segments with SWT < 3 mm (mean – 2SD) were considered dysfunctional¹⁸. Functional improvement was defined as increase in SWT of ≥ 1.5 mm, based on the in-plane spatial resolution of the cine sequence. LV volumes were normalized to the body surface area (m²).

Evaluation of contrast-enhanced images. Hyperenhancement was assessed by thresholding the images at 5 SD above the signal intensity of the remote, normal myocardium. Myocardial tissue showing a signal intensity of at least the threshold value was considered scar. Areas of hyperenhancement were quantified by computer-assisted planimetry on each of the short axis images and segmental extent of hyperenhancement (SEH, expressed as percentage of segmental area) was calculated.

Statistics

All data were expressed as mean \pm SD. For comparison of two data sets, paired or unpaired Student's *t* tests were performed where appropriate. Comparison of multiple data sets was performed using analysis of variance (ANOVA), specific differences were identified by a Student's *t* test corrected for multiple comparisons with Bonferroni inequality adjustment. Receiver operator characteristics (ROC) analysis for the differentiation between viable and nonviable segments by PTI and DCE was performed. Area under the ROC curve (AUC) was computed for both techniques. A *p* value < 0.05 was considered significant.

RESULTS

Fourteen patients completed the study protocol. All scans were of good quality.

Segmental analysis

One hundred and forty segments (10 segments per patient) were available for analysis. Fifty-five segments were normokinetic at baseline, 39 of these segments showed no hyperenhancement and were considered control segments. Sixteen segments with normal wall thickening at baseline (3.7 ± 0.9 mm) showed contrast-enhancement (mean SEH $22 \pm 20\%$), PTI in these segments was 1.03 ± 0.25 . Eighty-five segments with wall thickening of less than 3 mm were considered dysfunctional at baseline. Baseline segmental PET and MRI data are summarized in Table 2. There was a gradual decrease in PTI with increasing transmural extent of DCE ($p < 0.001$ by ANOVA).

Table 2. Baseline segmental PET and MRI data

	Control (n = 39)	Segmental extent of hyperenhancement Dysfunctional segments, n = 85				
		0% (n = 17)	1 - 25% (n = 34)	26 - 50% (n = 16)	51 - 75% (n = 8)	76 - 100% (n = 10)
EDWT	7.3 ± 2.5	8.3 ± 2.7	7.7 ± 2.4	7.0 ± 1.8	4.8 ± 2.0	5.7 ± 1.9
WTH	4.5 ± 1.2	1.6 ± 1.0	1.3 ± 1.0	0.9 ± 1.3	0.4 ± 1.0	0.8 ± 1.0
PTI	0.97 ± 0.18	1.15 ± 0.20	1.01 ± 0.20	0.98 ± 0.28	0.82 ± 0.25	0.70 ± 0.11

EDWT = End-Diastolic Wall Thickness (mm). WTH = Wall Thickening (mm). PTI = Perfusable Tissue Index.

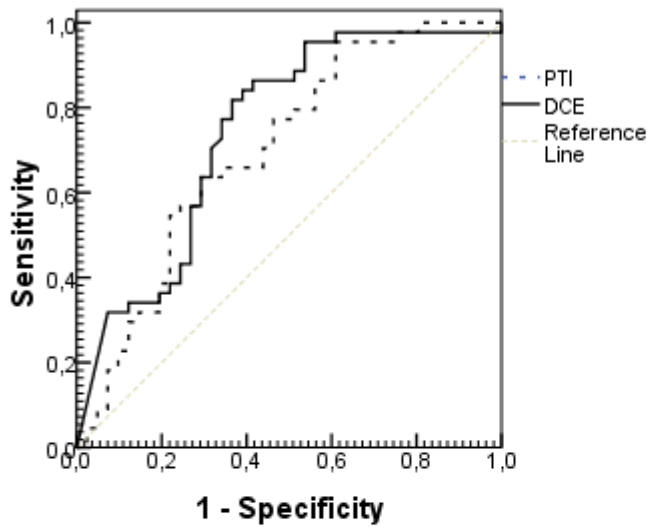


Figure 1. Receiver operator characteristics analysis of the differentiation between viable and non-viable segments by PET and MRI.

of 6 (17%) segments with 51-75% SEH and in 1 of 8 (13%) segments with 76-100% SEH. Mean PTI was 1.04 ± 0.20 in the improved segments vs. 0.90 ± 0.25 in the group without functional improvement ($p < 0.007$).

Receiver operator characteristics analysis of PTI and DCE MRI, predicting functional improvement after revascularization, is illustrated in Figure 1. The AUC's of PTI en DCE MRI were 0.70 and 0.74, respectively. There was no significant statistical difference between the AUC's. Cut-off value of 25% SEH for prediction of functional recovery after revascularization allowed us to correctly identify 82% segments with and 64% segments without reversible dysfunction. A threshold of 0.89 for PTI yielded the best diagnostic accuracy with sensitivity and specificity values of 76% and 54%, respectively.

Global function

At follow-up there was a significant decrease of mean LV dimensions and a moderate improvement of LVEF. These data are summarized in Table 3.

Table 3. Improvement of global function

	Baseline	Follow-up	
LVEDVi (mL/m ²)	121 ± 28	99 ± 24	$P = 0.02$
LVESVi (mL/m ²)	79 ± 28	61 ± 24	$P = 0.02$
LVEF (%)	35 ± 11	40 ± 11	$P = 0.05$
LVMi (g/m ²)	58 ± 15	59 ± 15	$P = 0.60$

LVEDVi: left ventricular end-diastolic volume indexed (to body surface area); LVESVi: left ventricular end-systolic volume indexed; LVEF: left ventricular ejection fraction; LVMi: left ventricular mass indexed.

Seventy-eight out of the initially 85 dysfunctional segments were revascularized. Follow-up MRI revealed no new areas of hyperenhancement compared to baseline examination. Improvement of wall thickening occurred in 41 segments (53%). Functional improvement was seen in: 13 of 16 (81%) segments without hyperenhancement, 21 of 33 (64%) segments with 1-25% SEH, 5 of 15 (33%) segments with 26-50% SEH, 1

DISCUSSION

The present study demonstrated that PTI can identify viable myocardium and predict improvement in regional function after revascularization in patients with chronic ischemic LV dysfunction. In agreement with our previous report¹², the optimal PTI cut-off value equaled 0.89.

To date, only three studies have been published where functionally recoverable myocardium was identified using PTI before revascularization⁸⁻¹⁰. In two of these studies^{8;10}, a cut-off value of 0.70 yielded the best diagnostic accuracy, which is distinctly lower than the optimal threshold of 0.89, found in the present study. By comparison, the lower cut-off of 0.70 was 98% sensitive, but only 24% specific, predicting functional recovery. In the third report by Gerber et al.⁹ a PTI cut-off value of 0.90 yielded the best diagnostic accuracy with sensitivity of 75% and specificity of 86%. These findings are more in agreement with the results of the present study.

The specificity of PTI for prediction of functional improvement in this study equaled 54%, which is considerably lower than previous reports using PTI. This could be in part explained by a substantial number (31%) of presumably viable segments with no or minimal scar (< 25% SEH on DCE MRI) that did not improve after revascularization. On the other hand, PTI underestimates infarct size. PTI of normal myocardium should be close to unity. Assuming the non-perfused fraction to be scar tissue, the reduction of PTI is a measure of the amount of damaged myocardium. This is supported by a gradual decrease in PTI with increasing transmural extent of hyperenhancement by DCE MRI. However, according to our data, PTI underestimates infarct size, given the fact that in segments with (near) transmural scar, PTI was 0.70 ± 0.11 .

There were no significant statistical differences between PTI and DCE MRI techniques, when their accuracy in predicting segmental functional improvement was compared. The observed diagnostic accuracy is in agreement with pooled analysis of traditional viability imaging techniques¹⁹.

Limitations

This study has some limitations that should be acknowledged. First, a limited number of patients were evaluated. Second, data of several short axis slices were averaged to generate 6 basal and 6 midventricular segments. Although averaging of information obligatory causes some loss in detail, it may be less sensitive to misalignment that is always a potential source

of error in follow-up studies. Third, mean follow-up in our study was six months, what may be too short to allow all potential viable segments to recover. However, at the same time less disease progression might have occurred. Furthermore, unlike DCE MRI, PTI measurements are not likely to become clinically applicable due to its complicated dynamic, multi-tracer imaging protocol. Recent developments in PET imaging, however, have enabled to generate parametric perfusion and PTI images^{20;21} without the use of a separate oxygen-15-labeled carbon monoxide scan. These developments should facilitate the use of PTI as a myocardial viability marker in conjunction with oxygen-15-labeled water perfusion myocardial PET scans. Future studies investigating comparative outcome and cost effectiveness of both techniques are needed.

CONCLUSION

Perfusable tissue index can identify viable myocardium and predict improvement in regional function after revascularization in patients with chronic ischemic LV dysfunction. The best diagnostic accuracy for PTI was achieved using a cut-off value of 0.89.

REFERENCES

1. Allman KC, Shaw LJ, Hachamovitch R, Udelson JE. Myocardial viability testing and impact of revascularization on prognosis in patients with coronary artery disease and left ventricular dysfunction: a meta-analysis. *J Am Coll Cardiol* 2002;39:1151-8.
2. Kim RJ, Fieno DS, Parrish TB, Harris K, Chen EL, Simonetti O et al. Relationship of MRI delayed contrast enhancement to irreversible injury, infarct age, and contractile function. *Circulation* 1999;100:1992-2002.
3. Kim RJ, Wu E, Rafael A, Chen EL, Parker MA, Simonetti O et al. The use of contrast-enhanced magnetic resonance imaging to identify reversible myocardial dysfunction. *N Engl J Med* 2000;343:1445-53.
4. Van HL, Vanderheyden M. Ischemic cardiomyopathy: value of different MRI techniques for prediction of functional recovery after revascularization. *AJR Am J Roentgenol* 2004;182:95-100.
5. Wellnhofer E, Olariu A, Klein C, Grafe M, Wahl A, Fleck E et al. Magnetic resonance low-dose dobutamine test is superior to SCAR quantification for the prediction of functional recovery. *Circulation* 2004;109:2172-4.
6. Selvanayagam JB, Kardos A, Francis JM, Wiesmann F, Petersen SE, Taggart DP et al. Value of delayed-enhancement cardiovascular magnetic resonance imaging in predicting myocardial viability after surgical revascularization. *Circulation* 2004;110:1535-41.
7. Yamamoto Y, de SR, Rhodes CG, Araujo LI, Iida H, Rechavia E et al. A new strategy for the assessment of viable myocardium and regional myocardial blood flow using 15O-water and dynamic positron emission tomography. *Circulation* 1992;86:167-78.
8. de Silva R, Yamamoto Y, Rhodes CG, Iida H, Nihoyannopoulos P, Davies GJ et al. Preoperative prediction of the outcome of coronary revascularization using positron emission tomography. *Circulation* 1992;86:1738-42.
9. Gerber BL, Melin JA, Bol A, Labar D, Cogneau M, Michel C et al. Nitrogen-13-ammonia and oxygen-15-water estimates of absolute myocardial perfusion in left ventricular ischemic dysfunction. *J Nucl Med* 1998;39:1655-62.
10. Itoh H, Namura M, Seki H, Asai T, Tsuchiya T, Uenishi H et al. Perfusable tissue index obtained by positron emission tomography as a marker of myocardial viability in patients with ischemic ventricular dysfunction. *Circ J* 2002;66:341-4.
11. Knaapen P, Boellaard R, Gotte MJ, van der Weerd AP, Visser CA, Lammertsma AA et al. The perfusable tissue index: a marker of myocardial viability. *J Nucl Cardiol* 2003;10:684-91.
12. Knaapen P, Bondarenko O, Beek AM, Gotte MJ, Boellaard R, van der Weerd AP et al. Impact of scar on water-perfusable tissue index in chronic ischemic heart disease: Evaluation with PET and contrast-enhanced MRI. *Mol Imaging Biol* 2006;8:245-51.
13. Knaapen P, Boellaard R, Gotte MJ, Dijkmans PA, van Campen LM, de Cock CC et al. Perfusable tissue index as a potential marker of fibrosis in patients with idiopathic dilated cardiomyopathy. *J Nucl Med* 2004;45:1299-304.
14. Iida H, Rhodes CG, de SR, Yamamoto Y, Araujo LI, Maseri A et al. Myocardial tissue fraction--correction for partial volume effects and measure of tissue viability. *J Nucl Med* 1991;32:2169-75.

15. Hermansen F, Rosen SD, Fath-Ordoubadi F, Kooner JS, Clark JC, Camici PG et al. Measurement of myocardial blood flow with oxygen-15 labelled water: comparison of different administration protocols. *Eur J Nucl Med* 1998;25:751-9.
16. Bondarenko O, Beek AM, Hofman MB, Kuhl HP, Twisk JW, van Dockum WG et al. Standardizing the definition of hyperenhancement in the quantitative assessment of infarct size and myocardial viability using delayed contrast-enhanced CMR. *J Cardiovasc Magn Reson* 2005;7:481-5.
17. van Ruge FP, van der Wall EE, Spanjersberg SJ, de RA, Matheijssen NA, Zwinderman AH et al. Magnetic resonance imaging during dobutamine stress for detection and localization of coronary artery disease. Quantitative wall motion analysis using a modification of the centerline method. *Circulation* 1994;90:127-38.
18. Bondarenko O, Beek AM, Nijveldt R, McCann GP, van Dockum WG, Hofman MB et al. Functional outcome after revascularization in patients with chronic ischemic heart disease: a quantitative late gadolinium enhancement CMR study evaluating transmural scar extent, wall thickness and periprocedural necrosis. *J Cardiovasc Magn Reson* 2007;9:815-21.
19. Schinkel AF, Bax JJ, Poldermans D, Elhendy A, Ferrari R, Rahimtoola SH. Hibernating myocardium: diagnosis and patient outcomes. *Curr Probl Cardiol* 2007;32:375-410.
20. Harms HJ, de HS, Knaapen P, Allaart CP, Lammertsma AA, Lubberink M. Parametric Images of Myocardial Viability Using a Single ^{15}O -H $_2\text{O}$ PET/CT Scan. *J Nucl Med* 2011;52:745-9.
21. Harms HJ, Knaapen P, de HS, Halbmeijer R, Lammertsma AA, Lubberink M. Automatic generation of absolute myocardial blood flow images using $[(^{15}\text{O})\text{H} (2)\text{O}]$ and a clinical PET/CT scanner. *Eur J Nucl Med Mol Imaging* 2011;38:930-9.

